APPLICATION OF THE NONLINEAR VORTEX-LATTICE CONCEPT TO AIRCRAFT-INTERFERENCE PROBLEMS

Osama A. Kandil, Dean T. Mook, and Ali H. Nayfeh
Virginia Polytechnic Institute and State University

SUMMARY

A discrete-vortex model is developed to account for the hazardous effects of the vortex trail issued from the edges of separation of a large leading wing on a small trailing wing. The model is divided into three main parts: the leading wing and its near wake, the near and far wakes of the leading wing, and the trailing wing and the portion of the far wake in its vicinity. The problem of the leading wing and its wake is solved by a nonlinear vortex-lattice technique which accounts for tip separation and the shape of the wake in the near and far fields. The trailing wing is represented by a conventional horseshoe-vortex lattice in which the tip separation and the shape of the wake are neglected. The solution is effected by iteration in a step-by-step approach. The normal-force, pitching-moment, and rolling-moment coefficients for the trailing wing are calculated. The circulation distribution in the vortex trail is calculated in the first part of the model where the leading wing is far upstream and hence is considered isolated. A numerical example is solved to demonstrate the feasibility of using this method to study interference between aircraft. The numerical results show the correct trends: The following wing experiences a loss in lift between the wing-tip vortex systems of the leading wing, a gain outside this region, and strong rolling moments which can change sign as the lateral relative position changes. All the results are strongly dependent on the vertical relative position.

INTRODUCTION

In recent years, there has been a significant increase in the use of wide-body and jumbo jets for civil air transports. The vortex trail associated with flying these heavy jets has high intensity and hence presents a serious hazard to small aircraft which enter this wake. Such a vortex encounter may produce high rolling moments on the trailing aircraft which could exceed the capability of the roll-control devices. In addition, the trailing aircraft could suffer a loss of altitude or climb rate and structural damage. The vortex trails may persist up to several miles and for long periods of time before they decay and dissipate by the action of atmospheric and viscous effects. Thus, they play a major factor in sequencing landing and take-off operations at airports where heavy and light aircraft are operating near each other (reference 1).

The vortices emanating from the wing tips of the leading aircraft roll up in the vicinity of the wing tips forming two helical-like cones of contra-rotating vortex cores. The strength of the vortex cores grows downstream from the leading edge up to the trailing edge. At the trailing edge, another wake emanates which has an increasing strength in the spanwise direction toward the wing tips (references 2-4). In the near wake beyond the trailing edge, the roll-up process continues and the strength of the trailing vortex grows due to the wake shed from the trailing edge. In the far wake, the core of the trailing vortex system increases and the vorticity decays with distance. When an aircraft originally with symmetric flow penetrates the wake, its freestream is no longer uniform; the flow may be asymmetric, depending on the aircraft position and orientation relative to this wake. In reference 5, three modes of penetration were reported. These modes, which are shown in figure 1, are called cross-track penetration, along-track penetration between vortices, and along-track penetration through the vortex center. Among these modes of penetration, it was shown that the third one is the most dangerous due to the rolling motion induced by the wake on the trailing airplane. This was calculated from an unsteady model of the trailing vortices in which vortex motion and decay were considered according to a two-dimensional model. Two equations based on a viscous vortex model were derived to calculate the change in lift and rolling-moment coefficients of the trailing aircraft wing from the undisturbed equilibrium flight condition (reference 6). In reference 7, a method was presented for predicting the geometry and the velocity field of a trailing vortex of an aircraft. The method is based on flight testing, model testing, and a solution of the Navier-Stokes equation for a two-dimensional axisymmetric flow. The results showed that the maximum tangential velocity in the core of the trailing vortex decreases with distance downstream of the generating aircraft. For large distances behind the aircraft, the decrease in this velocity was found to be inversely proportional to the square root of the distance. Moreover, the maximum tangential velocity and the corresponding core radius were found to be independent of the aircraft velocity.

DESCRIPTION OF THE PRESENT MODEL

In the present paper, we consider the three-dimensional flow to be steady, inviscid and irrotational everywhere except on the vortex lines which represent the wings and their wakes. This model was successfully applied to a short-coupled wing-wing configuration with delta planforms and leading-edge separations (reference 2). The full interaction between the wings and their wakes was considered, the shape of the wakes was determined, and the aerodynamic loads were calculated. It was found that when the trailing wing is at a distance equal to or larger than one-half the root chord of the leading wing, as measured from the trailing edge of the leading wing to the nose of the trailing wing, the aerodynamic loads of the leading wing are practically unaffected by the presence of the trailing wing. This leads to the conclusion that in the case of long-coupled wing-wing configurations or in the case of a trailing aircraft penetrating the wake of the leading aircraft, the model of the aerodynamic interaction can be simplified without any appreciable error in predicting the aerodynamic characteristics. This suggests modeling the flow field in the

following three steps: In the first step, we consider the leading wing and its trailing vortex system as an isolated aerodynamic problem similar to the one in references 2 and 3. In this step, the shape of the wake is determined as part of the solution up to a distance of two chords beyond the trailing edge. The rest of the wake beyond this distance is considered to be parallel to the freestream velocity. The circulation distribution in the wake is also found from this step and kept the same through the next two steps. In the second step, we consider the interaction between the near wake represented by the two chords beyond the trailing edge and the rest of the far wake in a step-by-step technique, marching downstream in each step. In this way, the wake of the leading wing can be carried downstream to any distance until it encounters the trailing wing. In the third step, we let the trailing wing interact with the vortex trail of the leading wing over a certain distance determined by the ratio of the root chord of the leading wing to that of the trailing wing. Here, the trailing wing may encounter a symmetric or an asymmetric flow, depending on its position and orientation with respect to the vortex trail. In the present study, we considered the along-tract penetration mode, including penetrations between the vortices, through the vortex center,and outside the vortices.

Although the present model does not account for the growth of the vortex core and the vortex decay,it represents a realistic approach for the three-dimensional inviscid solution which may be considered for further modifications to account for the viscous effects and the flow unsteadiness as well.

THE METHOD OF SOLUTION

The present model consists of three main parts. The first part includes the leading wing and its near wake, the second part includes the near and far wakes, and the third part includes the trailing wing and the portion of the far wake in its vicinity.

In the first part, we imagine the leading wing and its wake to be a vortex sheet, and we use a series of discrete vortex lines to represent these sheets. For the lifting surface, these lines form a lattice; while for the wake, they are nonintersecting. The segments connecting the points of intersection in the lattice are straight. Each line representing the wake is composed of a series of short straight segments and one final, semi-infinite segment. The short straight segments are used in two chord lengths beyond the trailing edge. Altogether the finite segments are used for three chord lengths, because the lifting surface itself is included.

Associated with each element of area in the lattice and with each finite segment in the wake is a control point. For the elements of area, the control point is the average of the four corners; for the finite segments in the wake, the control point is the upstream end.

The disturbance velocity generated by the discrete vortex segments is calculated according to the Biot-Savart law. Thus, the total velocity field, which is composed of the freestream and the disturbance, satisfies the continuity

equation for incompressible flows. The circulations around each vortex segment and the positions of the finite segments in the wake must be determined so that simultaneously the normal component of the total velocity vanishes at each control point on the lattice, circulation is spatially conserved, and each finite segment in the wake is force-free (when the finite segments are aligned with the total velocity at their control points, they are practically force-free). To effect this, we use the iteration scheme given in references 2-4. The results of this step are the shape of the wakes emanating from the wing tips and trailing edge as well as the circulation distribution. In this part, the positions and strengths of the finite segments in only two chord lengths behind the trailing edge are of interest.

The fact that the disturbance dies out rapidly in the upstream direction is the basis for the scheme used to determine the position of the wake at large distances behind the leading wing in the second part of the model. It is essential that this position be determined before the trailing wing is considered in the third part of the model. To effect this, we move downstream in steps, considering three chord lengths of finite segments at a time, and iterating to align only the segments in the two downstream chord lengths with the total velocity. At each step, one chord length of finite segments is added downstream and one is removed upstream. The result is the positions of the finite segments in both the near and far wakes. The presence of the trailing wing disturbs the wake from the leading wing, but this disturbance dies out rapidly in the upstream direction (reference 2). Thus, for the third part of the model, only those finite segments in two chord lengths in the vicinity of the trailing wing are of interest.

In the third part of the model, the trailing wing is a conventional large-aspect wing, and hence one can predict its total loads quite accurately by simply taking the vortex lines in its wake to be straight and ignoring the wing-tip vortex system. A number of horseshoe-vortex methods have been based on these simplifications; e.g. references 8-9. Obviously, these simplifications cannot be used when one wants to determine the distributed loads or a model of the wake.

To determine the circulation on the trailing wing, we use the following procedure. First, we select anchor points on each vortex line trailing from the leading wing which are upstream from the trailing wing and out of its region of influence. Then, we use the undisturbed position of the vortex lines from the leading wing as a guess for their position near the trailing wing and determine the circulations on it. Second, we calculate the total velocity field and, starting at the anchor points, align each finite segment in the lines from the leading wing with the total velocity at its control point. Then this position of the wake is used as the new guess and the procedure is repeated until the position converges.

The loads on the trailing wing are then calculated by summing the forces acting on the vortex segments and their moments. In contrast with the conventional horseshoe-lattice model, here there are significant forces on the legs of the horseshoe elements between the spanwise segments and the trailing edge which are produced by the cross flow induced by the vorticity in the wake of

the leading wing; these forces have been included. Many more details of the iterating scheme and many references related to the various models of the flow field and to experimental investigations of single wings are given in references 2 and 3.

NUMERICAL EXAMPLE

The method of solution outlined in the preceding section is implemented through three computer codes; each corresponds to one of the three parts of the model. In figure 2, we show a typical solution for the first two parts of the model. This includes the leading wing and the computed vortex lines representing its near and far wakes. The trailing wing is also shown. The drawing is to scale. The portion of the far wake in the vicinity of the trailing wing is the first guess for the solution of the third part. The aspect ratio of the leading wing (AR_ℓ) is seven; it is tapered, the sweep-back angle of the leading edge being twenty degrees and that of the trailing edge being ten degrees. The trailing wing is rectangular; its aspect ratio (AR_t) is six. The root chord of the leading wing $(c_r)_\ell$ is three times that of the trailing wing $(c_r)_t$. The coordinates (X_0,Y_0,Z_0) give the relative position of the trailing wing. For all the results presented below, the angle of attack is ten degrees for both wings and $X_0/(c_r)_\ell$ is 9.25.

In figure 3, we show the influence of the normal separation $Y_0/(c_r)_\ell$ on the normal-force coefficients (C_n) for four values of the lateral separation $(Z_0/c_r)_\ell$. The corresponding curves of the pitching-moment (C_{mz}) and rolling-moment (C_{mx}) coefficients are shown in figures 4 and 5, respectively. The results show that the load coefficients are very strongly dependent on the normal and lateral separations between the trailing and leading wings. The maximum increase and the minimum decrease in the load coefficients occur when the trailing wing is one to two chord lengths above the leading wing. This range includes the core of the vortex trail. In the lateral direction, the vortex core is located between two and three chord lengths from the plane of symmetry of the leading wing. When the trailing wing executes along-track penetration between the vortex cores, it suffers a loss in lift due to the downwash generated by the contra-rotating vortex cores. On increasing the lateral separation, the wing gains lift as it passes outside the vortex cores. The same trend occurs in the pitching-moment coefficients. But, the rolling-moment coefficient changes from a positive value to a negative one (figure 6). These effects can cause a serious hazard to the trailing aircraft.

The anomalies in the region near $Z_0 = 0$ are probably due to round-off errors caused by some vortex segments getting very close to a control point. These can be eliminated in a number of ways: e.g., one can multiply the velocity predicted by the Biot-Savart law by a pseudo-viscous term which renders the velocity zero on the vortex line and nearly equal to that predicted by the

Biot-Savart law a short distance away (ref. 10), or one can put a "rigid-body" finite core along the vortex segment (ref. 11), or one can use small lengths for the vortex segments so that the ratio of the distance from the segment to the length of the segment is never small.

The present results apparently show the correct trends and are in qualitative agreement with the results of reference 6.

CONCLUDING REMARKS

We have demonstrated the feasibility of using a discrete-vortex method to model aerodynamic interference. Such a method has several desirable features. As a result of the way the wake from the leading wing is determined, one can predict the influence of the leading-wing planform on any trailing wing. Moreover, the method can be extended to include the tip-vortex system of the trailing wing. The growth of the vortex core and vortex decay can be accounted for by including a viscous core similar to that of reference 7. Finally, an unsteady model, which takes into account the relative motion between the two wings, can be developed by using the technique of reference 12.

REFERENCES

1. McGowan, W. A.: Trailing Vortex Hazard. SAE Transactions, Vol. 77, 1968, pp. 740-753.

2. Kandil, O. A.: Prediction of the Steady Aerodynamic Loads on Lifting Surfaces Having Sharp-Edge Separation. Ph. D. Dissertation, Virginia Polytechnic Institute and State University, December 1974.

3. Kandil, O. A., Mook, D. T. and Nayfeh, A. H.: Nonlinear Prediction of the Aerodynamic Loads on Lifting Surfaces. Journal of Aircraft, Vol. 13, No 1, January 1976, pp. 22-28.

4. Kandil, O. A., Mook, D. T. and Nayfeh, A. H.: New Convergence Criteria for the Vortex-Lattice Models of the Leading-Edge Separation. Presented at NASA-Langley Workshop on Vortex-Lattice Utilization, May 1976. (To appear in a forthcoming NASA SP).

5. Wetmore, J. W. and Reeder, J. P.: Aircraft Vortex Wakes in Relation to Terminal Operations. NASA TN D-1777.

6. Iversen, J. D. and Bernstein, S.: Trailing Vortex Effects on Following Aircraft. Journal of Aircraft, Vol. 11, No. 1, January 1974, pp. 60-61.

7. McCormick, B. W., Tangler, J. L. and Sherrieb, H. E.: Structure of Trailing Vortices. Journal of Aircraft, Vol. 5, No. 3, May-June 1968, pp. 260-267.

8. Rubbert, P. E.: Theoretical Characteristics of Arbitrary Wings by a Nonplanar Vortex Lattice Method. Boeing Company, Seattle, Washington, Rept. D6-9244, 1962.

9. Hedman, S. G.: Vortex Lattice Method for Calculation of Quasi-Steady-State Loadings on Thin Elastic Wings. Aeronautical Research Institute of Sweden, Stockholm, Rept. 105, 1966.

10. Yager, P. M., Holland, C. G., Jr. and Strand, T.: Modified Weissinger Lifting Surface Method for Calculating Aerodynamic Parameters of Arbitrary Wing-Canard Configurations. Air Vehicle Corporation, La Jolla, California, Report No. 354, 1967.

11. Scully, M. P.: A Method of Computing Helicopter Vortex Wake Distortion. Massachusetts Institute of Technology, Aeroelastic and Structure Research Laboratory, ASRL TR-138-1, 1967.

12. Atta, E. H., Kandil, O. A., Mook, D. T. and Nayfeh, A. H.: Unsteady Flow Past Wings Having Sharp-Edge Separation. Presented at NASA-Langley Workshop on Vortex-Lattice Utilization, May 1976. (To appear in a forthcoming NASA SP).

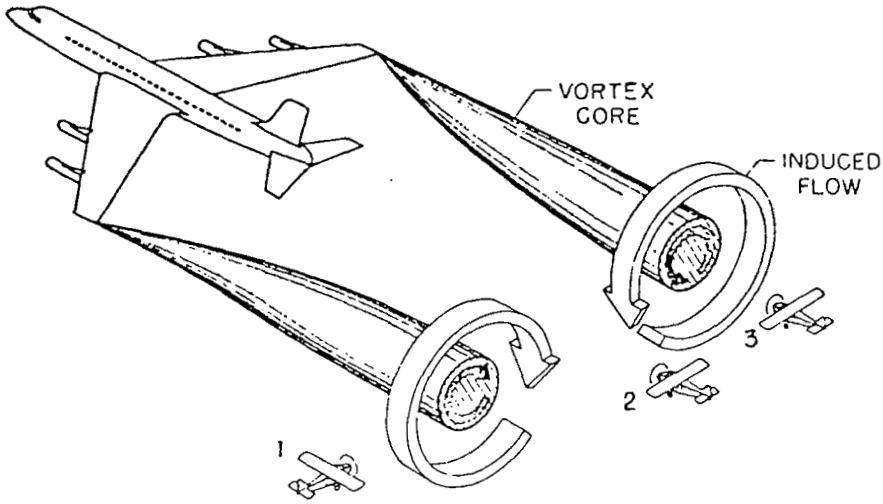

Figure 1.- Illustration of trailing vortex wake and types of encounter (from ref. 5): cross-track penetration (1), along-track penetration between vortices (2), and along-track penetration through vortex center (3).

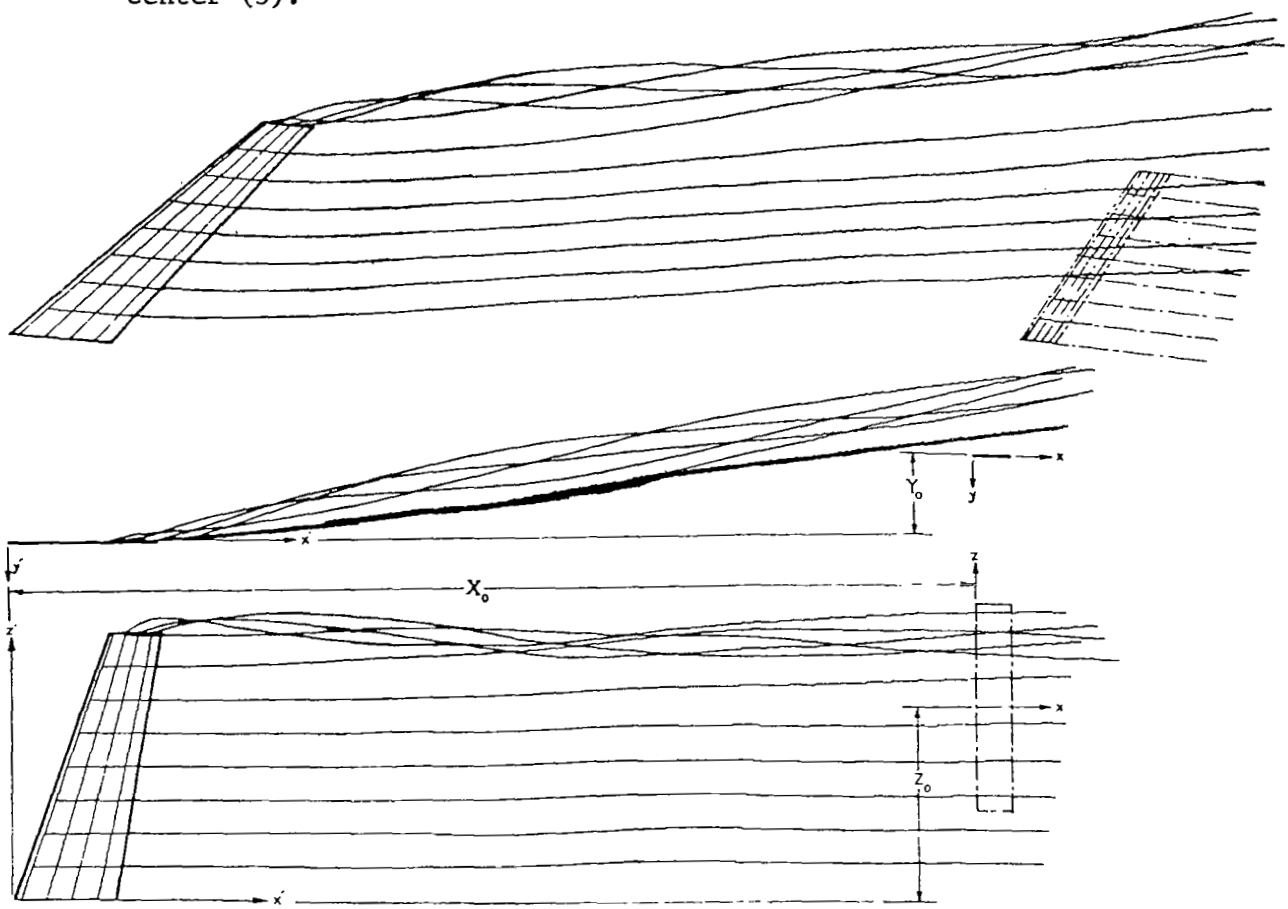

Figure 2.- Typical solution of the near and far wakes of the leading wing. Angle of attack = 10°; AR_{ℓ} = 7; 4 × 8 lattice.

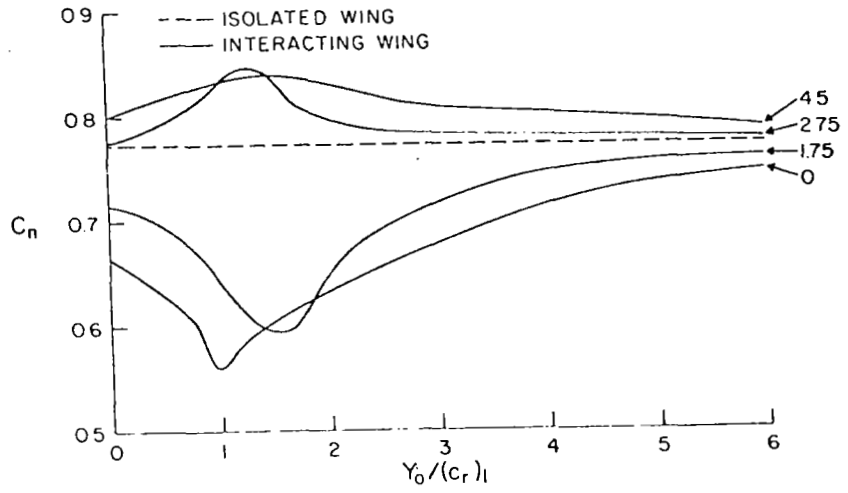

Figure 3.- Normal-force coefficient vs. normal separation above the leading wing for various lateral separations $Z_0/(c_r)_\ell$. $X_0/(c_r)_\ell = 9.25$; $AR_\ell = 7$; $AR_t = 6$; $(c_r)_\ell/(c_r)_t = 3$.

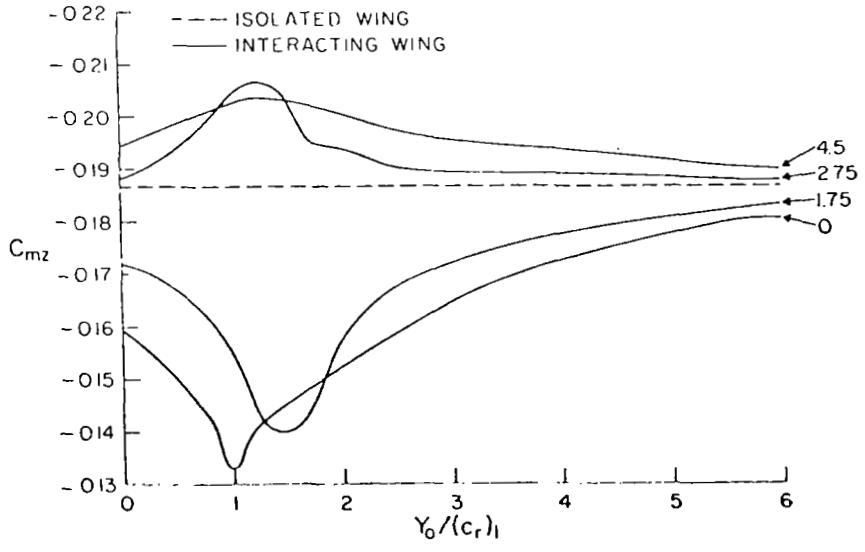

Figure 4.- Pitching-moment coefficient vs. normal separation above the leading wing for various lateral separations $Z_0/(c_r)_\ell$. $X_0/(c_r)_\ell = 9.25$; $AR_\ell = 7$; $AR_t = 6$; $(c_r)_\ell/(c_r)_t = 3$.

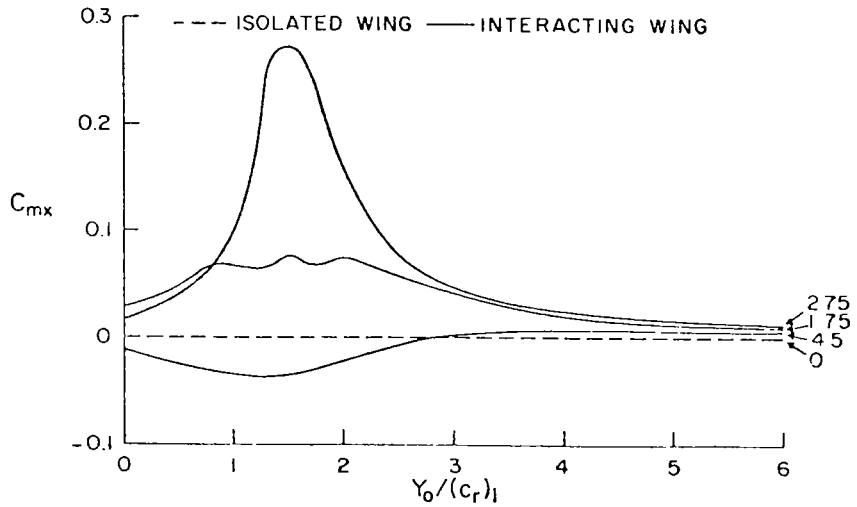

Figure 5.- Rolling-moment coefficient vs. normal separation above the leading wing for various lateral separations $Z_0/(c_r)_\ell$. $X_0/(c_r)_\ell = 9.25$; $AR_\ell = 7$; $AR_t = 6$; $(c_r)_\ell/(c_r)_t = 3$.

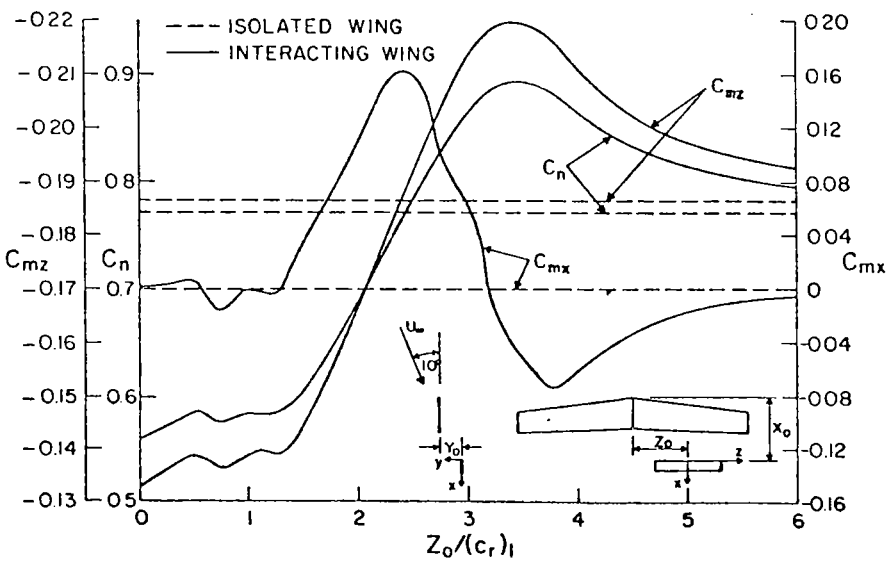

Figure 6.- Normal-force (C_n), pitching-moment (C_{mz}), and rolling-moment (C_{mx}) coefficients vs. lateral separation. $X_0/(c_r)_\ell = 9.25$; $Y_0/(c_r)_\ell = 1$; $AR_\ell = 7$; $AR_t = 6$; $(c_r)_\ell/(c_r)_t = 3$.